Journal of Alloys and Compounds 509 (2011) 157–160

Contents lists available at ScienceDirect

Journal of Alloys and Compounds

journal homepage: www.elsevier.com/locate/jallcom

Fabrication of highly ordered porous nickel phosphide film and its electrochemical performances toward lithium storage

J.Y. Xiang, X.L. Wang*, X.H. Xia, J. Zhong, J.P. Tu*

State Key Laboratory of Silicon Materials, Department of Materials Science and Engineering, Zhejiang University, Hangzhou 310027, China

ARTICLE INFO

Article history:
Received 26 June 2010
Received in revised form 30 August 2010
Accepted 1 September 2010
Available online 15 September 2010

Keywords:
Nickel phosphide
Porous film
Electrodeposition
Anode
Lithium ion battery

ABSTRACT

Highly ordered porous Ni_3P film was successfully electrodeposited through a self-assembled monodisperse polystyrene sphere template on copper substrate after heat treatment. The spherical pores left in the film after the removal of polystyrene spheres are well-ordered and close-packed. The diameter of the pores arranged in the film is about 800 nm and the thickness of the wall connecting adjacent pores is 60 nm. As anode for lithium ion batteries, the nanostructured porous Ni_3P film exhibits improved capability and reversibility over the dense one. After 50 cycles, the reversible capacity of the porous Ni_3P film is 403 mAh g^{-1} and 239 mAh g^{-1} at 0.2 C and 2 C, maintaining 78.1% and 67.9% of the capacity in the 2nd cycle, respectively. The enhanced electrochemical performance of the porous film is attributed to the better contact between Ni_3P and electrolyte, which provides more sites for Li^+ accommodation, shortens the diffusion length of Li^+ and enhances the kinetics of electrode process. Moreover, the porous structure is stable and can sustain well even after 50 cycles.

1. Introduction

For the last decade, many efforts have been devoted to improving the conversion efficiency and cycling performance of anodes for lithium ion batteries. A promising approach is reducing the polarization and enhancing the kinetics of electrode process [1–8]. Among the various anode materials such as carbonaceous material, intermetallic compounds, transition metal oxides and phosphides (*M*–O and *M*–P, where *M* = Fe, Co, Ni, Cu, etc.), transition metal phosphides attract much attention due to their low polarization and good cycling stability [9–14]. However, most metal phosphides have to be obtained at high temperatures or under complex conditions such as hydrothermal synthesis for a long time [15–20]. Recently, our group has successfully prepared Ni_3P films by using a simple electrodeposition method [21]. Though the as-deposited film exhibits good electrochemical performance at a relative low rate, it can hardly deliver satisfied high-rate properties due to the dense structure. Hence, in the present work, we report a facile synthesis of highly ordered porous Ni_3P film by electrodeposition through a self-assembled monodisperse polystyrene sphere template after further heat treatment. The structure and morphology of the porous film are characterized and the improved electrochemical performances are investigated.

2. Experimental

2.1. Assembly of monolayer polystyrene sphere template

A small amount of polystyrene spheres with diameters of 800 nm were firstly dispersed in a mixture of ethanol and deionized water (volume rate is 3:1). Then, the suspension was dropped into deionized water prefilled in a Petri dish to form a monolayer of polystyrene spheres on the surface of water. A few drops of 2% dodecylsodiumsulfate solution were then added into the water, and the polystyrene spheres suspended on the surface of water were pushed aside and became tight. Next, chemical polished copper foil (99.9%) with a diameter of 12 mm was immersed into the water through the clear area and lifted up horizontally through the polystyrene sphere layer. Finally, a monodisperse polystyrene sphere layer was self-assembled on the surface of the copper foil.

2.2. Preparation and characterization of porous Ni_3P film

The porous Ni_3P film was electrodeposited in a three-electrode system using the copper substrate with polystyrene sphere template as the working electrode, a Pt foil as the counter electrode and a saturated calomel electrode (SCE) as the reference electrode. The bath consisted of 0.6 M $NiSO_4 \cdot 6H_2O$, 0.2 M $NiCl_2 \cdot 6H_2O$, 0.8 M H_3BO_3 and 0.6 M $NaH_2PO_4 \cdot H_2O$. The electrodepositing process was carried out at a current density of 0.02 A cm^{-2} at 55 °C for 5 min. Afterwards, the sample was immersed into toluene for 24 h to remove the polystyrene spheres. Finally, the as-prepared film was heated at 500 °C for 1 h under the flowing argon atmosphere and cooled with furnace to room temperature. For comparison, a dense Ni_3P film was also prepared by electrodeposition following the above procedures using a copper foil without template as the substrate.

The structure and morphology of the Ni_3P films were characterized by X-ray diffraction (XRD, Philips PC-APD with Cu Kα radiation) and field emission scanning electron microscopy (FESEM, FEI SIRON and Hitachi S-4700), respectively.

3. Electrochemical measurements

The galvanostatic charge–discharge tests of the Ni_3P films were investigated in a coin-type cell (CR 2025), which was assembled

* Corresponding authors. Tel.: +86 571 87952856; fax: +86 571 87952573.
E-mail addresses: wangxl@zju.edu.cn (X.L. Wang), tujp@zju.edu.cn (J.P. Tu).

0925-8388/$ – see front matter © 2010 Elsevier B.V. All rights reserved.
doi:10.1016/j.jallcom.2010.09.013

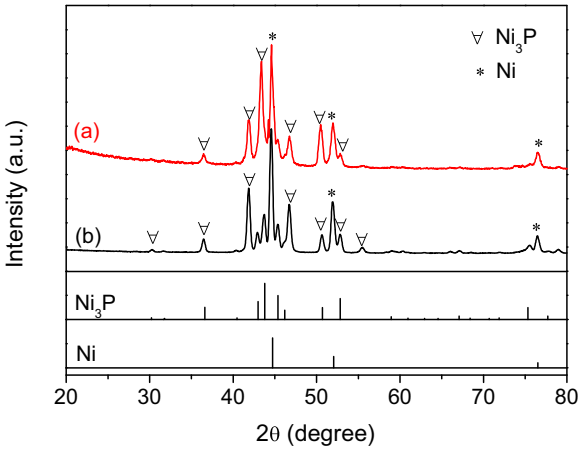

Fig. 1. XRD patterns of the electrodeposited films after heat treatment: (a) with and (b) without using polystyrene sphere template.

following the procedures in Ref. [22] and conducted on LAND battery program-control test system at different rates from 0.02 V to 3.0 V (versus Li/Li^+) at room temperature (25 ± 1 °C). Electrochemical impedance spectrum (EIS) was performed on CHI660C electrochemical workstation. The test cell was a particular three-electrode glass cell using the as-prepared Ni_3P film as working electrode, and lithium foils as both the counter and reference electrodes. The EIS measurement was carried out in the frequency range from 100 kHz to 10 mHz under AC stimulus with 5 mV of amplitude and no applied voltage bias.

4. Results and discussion

The XRD patterns of the electrodeposited films after heat treatment are shown in Fig. 1. Tetragonal Ni_3P (I4 space group, JCPDS 34-0501) is the main phase in both the films prepared with and without polystyrene sphere template. Besides, metallic Ni is detected as a side product. Although the as-deposited Ni_3P film is not a pure one, the side product nickel will play a positive role (facilitate the decomposition of Li_3P and make the charge reaction $3Ni + Li_3P \Leftrightarrow Ni_3P + 3Li^+ + 3e^-$ proceed to a higher extent) when the film is used as anode for lithium ion batteries. It has been discussed intensively in our previous work [21].

Fig. 2a presents the SEM image of the Ni_3P film electrodeposited through the polystyrene sphere template. It is shown that the spherical pores left in the film after the removal of polystyrene spheres are well-ordered, close-packed and with the same diameter as the polystyrene spheres (about 800 nm). The thickness of the wall connecting adjacent pores is about 60 nm. From the cross-sectional view (inset of Fig. 2a), it is observed that the ordered pores arranged in the film look like open bowls and the thin walls of these bowls make up a three-dimensional network nanostructure. Moreover, the thickness of the porous Ni_3P film is also about 800 nm. It is thus concluded that the morphology of the porous film is greatly influenced by the polystyrene sphere template. If polystyrene spheres with smaller diameter are used as the template, porous film with more tiny nanostructure will be obtained. The Ni_3P film electrodeposited without using template is quite dense and the thickness of the film is about 1 μm (Fig. 2b). The loading weights of the porous and dense Ni_3P film are 0.65 mg cm^{-2} and 1.08 mg cm^{-2}, respectively.

The first discharge–charge curves for the porous and dense Ni_3P films at a rate of 0.2 C (1 C = 388 mA g^{-1}) from 0.02 V to 3.0 V are given in Fig. 3. The electrochemical behaviors toward Li^+ are a little different between the two electrodes. For the porous Ni_3P film, the discharge plateau that corresponds to the electrode reaction

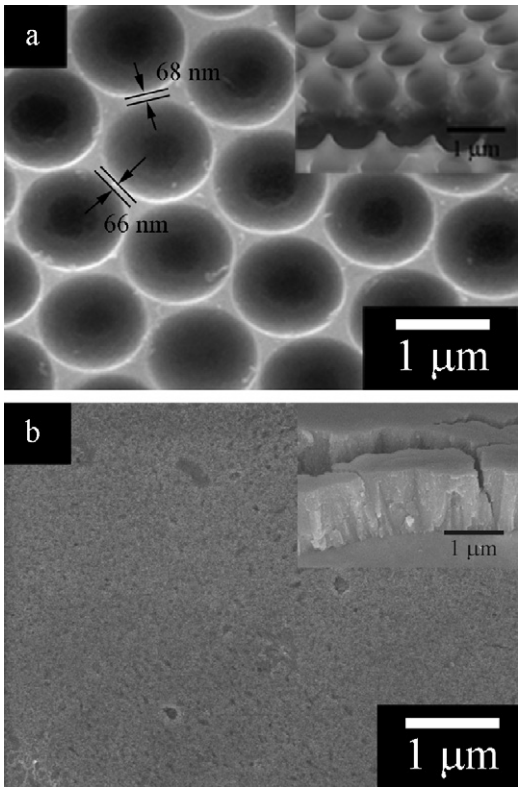

Fig. 2. SEM images of the electrodeposited Ni_3P films after heat treatment: (a) with and (b) without using polystyrene sphere template.

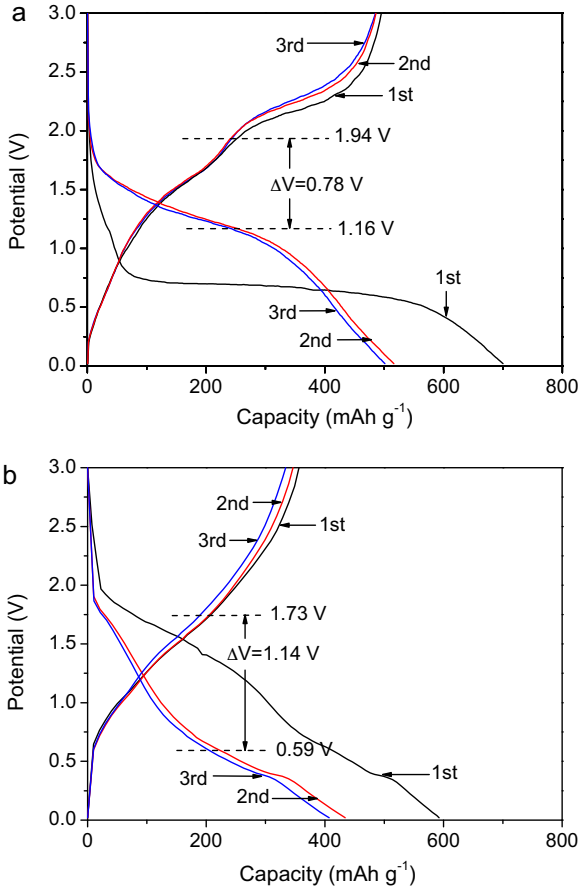

Fig. 3. The first discharge–charge curves of (a) porous and (b) dense Ni_3P film in the voltage range of 0.02–3.0 V (versus Li/Li^+) at 0.2 C.

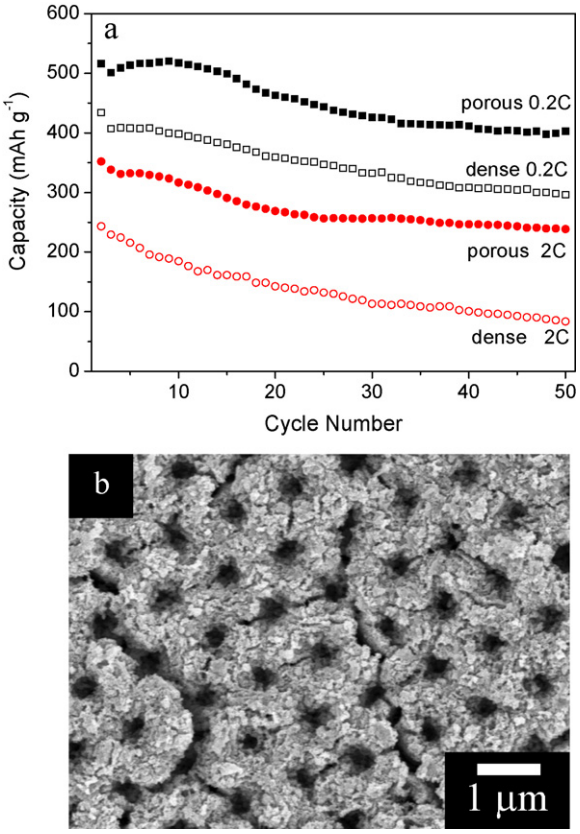

Fig. 4. (a) Cycling performances of the Ni_3P films at rates of 0.2 C and 2 C (from the 2nd to the 50th cycle), (b) SEM image of the porous Ni_3P film after 50 cycles at a rate of 0.2 C.

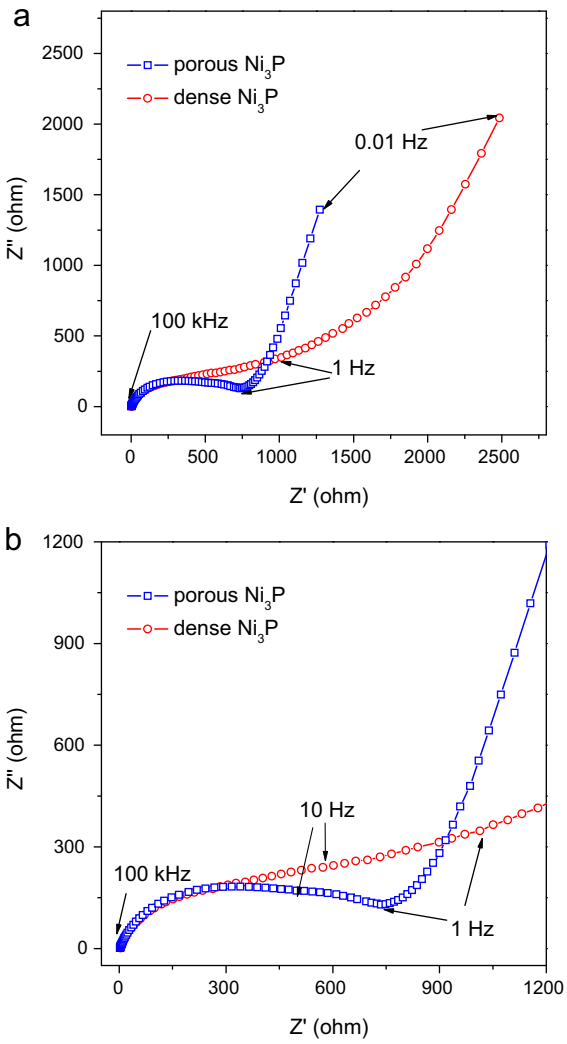

Fig. 5. Nyquist plots of the Ni_3P electrodes in the frequency range from 0.01 Hz to 100 kHz after discharging the electrodes to 0.02 V in the 5th cycle.

$Ni_3P + 3Li + 3e^- \Leftrightarrow Li_3P + 3Ni$ is flat and locates at 0.7 V. However, for the dense film, except for the plateau at 0.7–0.5 V, another long inclined plateau appears at 1.9–1.2 V in the first discharge curve, which does not appear in the curve of porous Ni_3P. According to Ref. [21], this plateau should be ascribed to the formation of an intermediate compound $Ni_{12}P_5$. Thus, it is considered that the porous Ni_3P exhibits a one-step electrode reaction process in the first discharge process, while the dense film delivers a two-step reaction process, including the formation of intermediate compound $Ni_{12}P_5$ and the further transformation to Li_3P and Ni.

In the subsequent cycles, the discharge plateau of porous Ni_3P film shifts to a higher voltage (about 1.2 V) and becomes a little inclined. But for the dense Ni_3P film, the discharge plateaus in the first and subsequent cycles are almost at the same location. The interval between the discharge and charge plateaus indicates the polarization of the electrode. Since the discharge and charge plateaus are inclined, it is hard to point out what voltages are exactly corresponding to the plateaus. Hence, midpoint voltages (the battery voltage at the midpoint charge–discharge capacity) are used to investigate the polarization of the electrode. Obviously, the interval between the discharge and charge midpoint voltages of the porous Ni_3P film ($\Delta V = 0.78$ V) is much smaller than that of the dense one ($\Delta V = 1.14$ V), which indicates the weaker polarization of the porous Ni_3P electrode. One of the main causes for the electrode polarization is the transferring delay of electrons and lithium ions on active material/electrolyte interfaces [23]. Therefore, it is considered that the electrons and lithium ions can transfer more actively in the nanostructured porous film due to the better contact between Ni_3P and electrolyte.

In addition, the first irreversible capacities of the porous and dense Ni_3P electrodes are 184 mAh g^{-1} and 158 mAh g^{-1}, respectively. The initial capacity loss commonly reflects the formation of large-scale SEI during the discharging process and the incomplete decomposition in the subsequent charging process [1,24–27]. The capacity loss of porous Ni_3P film during the first cycle is a little larger than that of the dense one. It is explained that the electrode reaction is significantly enhanced owing to the larger contact area of Ni_3P and electrolyte in the nanostructured porous structure. Even though, in the 2nd cycle, the discharge capacity of the porous film is about 500 mAh g^{-1}, which is still much higher than that of the dense one.

The cycling performances of the porous and dense Ni_3P films at rate of 0.2 C and 2 C are shown in Fig. 4a. The porous Ni_3P film exhibits much better cyclability than the dense one, especially at high rate. At 0.2 C, the reversible capacities of the porous and dense Ni_3P films are 403 mAh g^{-1} and 296 mAh g^{-1} after 50 cycles, keeping 78.1% and 68.2% of those in the 2nd cycle, respectively. As the discharge–charge rate increases to 2 C, the reversible capacity of the porous Ni_3P film is 239 mAh g^{-1}, still keeping 67.9% of that in the 2nd cycle. However, for the dense Ni_3P film, the capacity is only 84 mAh g^{-1}, keeping 34.6% of that in the 2nd cycle. The improved capability and high-rate properties of the porous Ni_3P film is greatly attributed to the ordered porous nanostructure, which provides large contact area of active material and electrolyte. Therefore, the sites for Li^+ accommodation are increased, the diffusion length of Li^+ is shortened, and the electrode process kinetics is enhanced [28].

Fig. 4b presents the SEM image of the porous Ni_3P film after 50 cycles at 0.2 C. The porous structure sustains well though the pore wall becomes thicker and the surface is not as smooth as that before cycling. The stable porous nanostructure also indicates the excellent capacity retention of the porous Ni_3P film.

To further understand the mechanism for the improved cyclability of the porous Ni_3P film, EIS measurements were conducted in the frequency range from 0.01 Hz to 100 kHz after discharging the electrodes to 0.02 V (versus Li/Li^+) at 0.2 C in the 5th cycle. As is known to all, the high frequency region in the Nyquist plots is indexed to the migration impedance of lithium ions through the surface layer, the medium frequency region corresponds to the charge-transfer impedance in the film-solution interface, and the low frequency region reflects the solid-state diffusion impedance of lithium ions in the active material [29]. However, the Nyquist plots of both the porous and dense Ni_3P electrodes exhibit only a depressed semicircle in high-medium frequency region and a following 45° line in low frequency (as shown in Fig. 5). It is supposed that the high-frequency semicircle ascribed to the migration of Li^+ through the surface layer is too small to be detected and the depressed high-medium frequency semicircle in the Nyquist plots of the Ni_3P electrodes is mainly indexed to the charge-transfer resistance. As can be seen, the porous Ni_3P electrode shows a smaller high-medium frequency semicircle than the dense one, which indicates the lithium ions and electrons can transfer more easily on Ni_3P/electrolyte interfaces in the porous structure rather than in the dense one. The decreasing charge-transfer resistance results in the enhanced electrode process kinetics and improved electrochemical performance of the porous Ni_3P film, especially at high rate.

5. Conclusions

Highly ordered porous Ni_3P film was prepared by electrodeposition through a self-assembled monodisperse polystyrene sphere template. By comparison with the dense film, the porous Ni_3P film exhibits higher reversible capacity, lower polarization and enhanced electrode process kinetics. After 50 cycles, the reversible capacity of the porous Ni_3P film maintains 403 mAh g^{-1} and 239 mAh g^{-1} at 0.2 C and 2 C, respectively. The excellent electrochemical performance is attributed to the porous nanostructure, which provides sufficient contact of Ni_3P/electrolyte and shortens the diffusion length of lithium ions. In addition, this simple and low-cost method provides a promising approach for fabricating other nanoporous transition metal phosphide films as anodes for next-generation lithium ion batteries.

References

[1] F. Gillot, S. Boyanov, L. Dupont, M.L. Doublet, M. Morcrette, L. Monconduit, Chem. Mater. 17 (2005) 6327–6337.
[2] J. Xu, H.R. Thomas, R.W. Francis, K.R. Lum, J. Wang, B. Liang, J. Power Sources 177 (2008) 512–527.
[3] X.H. Xia, J.P. Tu, J. Zhang, X.L. Wang, W.K. Zhang, H. Huang, ACS Appl. Mater. Interface 2 (2010) 186–192.
[4] R.G. Lv, J. Yang, P.F. Gao, Y.N. NuLi, J.L. Wang, J. Alloys Compd. 490 (2010) 84–87.
[5] Y.S. Lin, J.G. Duh, D.T. Shieh, M.H. Yang, J. Alloys Compd. 490 (2010) 393–398.
[6] Q.T. Pan, K. Huang, S.B. Ni, F. Yang, S.M. Lin, D.Y. He, J. Alloys Compd. 484 (2009) 322–326.
[7] J.Y. Xiang, J.P. Tu, J. Zhang, J. Zhong, D. Zhang, J.P. Cheng, Electrochem. Commun. 12 (2010) 1103–1107.
[8] J.Y. Xiang, X.L. Wang, X.H. Xia, L. Zhang, Y. Zhou, S.J. Shi, J.P. Tu, Electrochim. Acta 55 (2010) 4921–4925.
[9] D.C.C. Silva, O. Crosnier, G. Ouvard, J. Greedan, A. Safa-Sefat, L.F. Nazar, Electrochem. Solid-State Lett. 6 (2003) A162–A165.
[10] V. Pralong, D.C.S. Souza, K.T. Leung, L. Nazar, Electrochem. Commun. 4 (2002) 516–520.
[11] X.Y. Fan, F.S. Ke, G.Z. Wei, L. Huang, S.G. Sun, J. Alloys Compd. 476 (2009) 70–73.
[12] M. Cruz, J. Morales, L. Sanchez, J. Santos-Pena, F. Martin, J. Power Sources 171 (2007) 870–878.
[13] L.C. Yang, W.L. Guo, Y. Shi, Y.P. Wu, J. Alloys Compd. 501 (2010) 218–220.
[14] C.Q. Zhang, J.P. Tu, X.H. Huang, Y.F. Yuan, X.T. Chen, F. Mao, J. Alloys Compd. 441 (2007) 52–56.
[15] Z.S. Zhang, J. Yang, Y.N. Nuli, B.F. Wang, J.Q. Xu, Solid State Ionics 176 (2005) 693–697.
[16] M.P. Bichat, T. Politova, H. Pfeiffer, F. Tancret, L. Monconduit, J.L. Pascal, T. Brousse, F. Favier, J. Power Source 136 (2004) 80–87.
[17] X. Wang, F. Wan, J. Liu, Y. Gao, K. Jiang, J. Alloys Compd. 474 (2009) 233–236.
[18] L. Takacs, S.K. Mandal, Mater. Sci. Eng. A 304–306 (2001) 429–433.
[19] X. Chen, S. Yamanaka, J. Alloys Compd. 370 (2004) 110–113.
[20] X.J. Wang, F.Q. Wan, J. Liu, Y.J. Gao, K. Jiang, J. Alloys Compd. 474 (2009) 233–236.
[21] J.Y. Xiang, J.P. Tu, X.L. Wang, X.H. Huang, Y.F. Yuan, X.H. Xia, Z.Y. Zeng, J. Power Sources 185 (2008) 519–525.
[22] X.H. Huang, J.P. Tu, X.H. Xia, X.L. Wang, J.Y. Xiang, L. Zhang, Y. Zhou, J. Power Sources 188 (2009) 588–591.
[23] D. Aurbach, B. Markovsky, I. Weissman, E. Levi, Y. Ein-Eli, Electrochim. Acta 45 (1999) 67–86.
[24] H. Wang, Q. Pan, J. Zhao, W. Chen, J. Alloys Compd. 476 (2009) 408–413.
[25] K. Wang, J. Yang, J. Xie, B. Wang, Z. Wen, Electrochem. Commun. 5 (2003) 480–483.
[26] S. Boyanov, J. Bernardi, F. Gillot, L. Dupont, M. Womes, J.M. Tarascon, L. Monconduit, M.L. Doublet, Chem. Mater. 18 (2006) 3531–3538.
[27] X.H. Huang, J.P. Tu, Y.Z. Yang, J.Y. Xiang, Electrochem. Commun. 10 (2008) 16–19.
[28] J.Y. Xiang, J.P. Tu, L. Zhang, Y. Zhou, X.L. Wang, S.J. Shi, J. Power Sources 195 (2010) 313–319.
[29] M.D. Levi, D. Aurbach, J. Phys. Chem. B 101 (1997) 4630–4640.